The Tumor Suppressor SCRIB is a Negative Modulator of the Wnt/β-Catenin Signaling Pathway

Avais M Daulat, Mônica Silveira Wagner, Alexandra Walton, Emilie Baudelet, Stéphane Audebert, Luc Camoin, Jean-Paul Borg

The tumor suppressor SCRIB is a negative modulator of the Wnt/β-catenin signaling pathway

Avais M. Daulat[1,§], Mônica Silveira Wagner[1,§], Alexandra Walton[1], Emilie Baudelet[2], Stéphane Audebert[2], Luc Camoin[2,#,*], Jean-Paul Borg[1,2,#,*]

[1]Centre de Recherche en Cancérologie de Marseille, Equipe labellisée Ligue 'Cell polarity, cell signaling and cancer', Aix-Marseille Université, Inserm, CNRS, Institut Paoli Calmettes, 13009 Marseille, France

[2]Centre de Recherche en Cancérologie de Marseille, Marseille Proteomics, Aix-Marseille Université, Inserm, CNRS, Institut Paoli Calmettes, 13009 Marseille, France

* To whom correspondence should be addressed: luc.camoin@inserm.fr/jean-paul.borg@inserm.fr/ Phone 33-4-8697-7201, Fax 33-4-8697-7499

§ Co-first authors

Co-lead authors

Keywords: SCRIB, LANO, tumor suppressor, cancer, Wnt

Abstract

SCRIB is a scaffold protein containing LRR and PDZ domains which localizes at the basolateral membranes of polarized epithelial cells. Deregulation of its expression or localization leads to epithelial defects and tumorigenesis in part as a consequence of its repressive role on several signaling pathways including AKT, ERK and HIPPO. In the present work, we used a proteomic approach to characterize the protein complexes associated to SCRIB and its paralogue LANO. We identified common and specific sets of proteins associated to SCRIB and LANO by mass spectrometry and provide an extensive landscape of their associated networks, and the first comparative analysis of their respective interactomes. Under proteasome inhibition, we further found that SCRIB was associated to the β-catenin destruction complex which is central in Wnt/β-catenin signaling, a conserved pathway regulating embryonic development and cancer progression. We show that the SCRIB/β-catenin interaction is potentiated upon Wnt3a stimulation and that SCRIB plays a repressing role on Wnt signaling. Our data thus provide evidence for the importance of SCRIB in the regulation of the Wnt/β-catenin pathway.

Statement of significance of the study

Epithelial cell polarity is organized and maintained by a set of PDZ domain containing proteins which includes SCRIB, a cytoplasmic scaffold with tumor suppressing functions. SCRIB belongs to the LAP protein family which also comprises LANO, a paralogue lacking PDZ domains. We set up an unbiased approach to identify the protein complexes associated to SCRIB and LANO by high-resolution mass spectrometry and provide their first in-depth comparative interactomes. Commonalities and differences of partners were found and future studies will benefit from this resource to further study the functions of these cell polarity components involved in cancer. We also demonstrated that SCRIB is physically and functionally associated to the Wnt/β-catenin complex, and acts as a negative regulator of Wnt/β-catenin as previously shown for LANO. The SCRIB-LANO branch of the LAP family is thus not only characterized by sequence and interactome commonalities but also by common signaling properties that may synergize in cancer development.

Introduction

Epithelial tissues are highly organized structures that rely on cell polarity pathways driven by membrane receptors and scaffolding proteins. SCRIB is a large cytoplasmic scaffold protein present at cell-cell junctions in polarized cells that contains LRR and PDZ domains and is a member of the LAP protein family. The family is composed of DENSIN-180, ERBIN, SCRIB and LRRC1/LANO (hereafter referred to as LANO). Based on phylogenic trees, LAP proteins can be split in two branches, one comprising SCRIB and LANO and the second one ERBIN and DENSIN-180 [1].

Loss of SCRIB in *Drosophila* and mammals leads to cell polarity defects and cancer development [2],[3]. In normal epithelial cells, SCRIB is recruited at the plasma membrane through E-cadherin engagement [4] and negatively regulates a set of signaling pathways including AKT [5], ERK [6] and HIPPO [7] pathways. SCRIB expression has been shown to regulate cell proliferation, as demonstrated by its tumor suppressor role in mouse mutants [8, 9]. It can also associate with oncogenic viral proteins such as human papilloma [10] or T lymphotropic viruses [11, 12] which promote its degradation or mislocalization. Furthermore, loss of SCRIB expression in conjunction with oncogenic activation of H-Ras [13] [14] or c-Myc [9] enhances cancer cell proliferation.

Epithelial organization is important for tissue homeostasis and relies on the self-renewal versus differentiation of stem cells which is directed by extrinsic short-ranged signals that emanate from the local environment. Wnt signaling is required to control cell differentiation and proliferation [15]. In cancer cells, Wnt signaling is often up-regulated and promotes cancer progression by enhancing cell proliferation [16]. At the molecular level, in the absence of Wnt, cytoplasmic β-catenin is constantly ubiquitinated and degraded by the proteasome. This process is governed by a molecular machinery called the β-catenin destruction complex. The destruction complex is composed of the scaffolding proteins Axin, APC, Dvl, Amer1 and

the protein kinases CK1α and GSK3α/β, and functions by catalyzing the serine/threonine phosphorylation of a conserved region at the N-terminus of β-catenin. This event promotes the recruitment of the β-TRCP1 E3-ubiquitin ligase and therefore leads to β-catenin proteasome-mediated degradation. The destruction complex is regulated by the secreted glycoprotein Wnt which binds to a plasma membrane heterodimer including a Frizzled (FZD) family member and one of the Wnt co-receptors, LRP5 or LRP6 (LRP5/6). Wnt binding to the FZD-LRP5/6 complex results in the successive recruitment of Dishevelled and the Axin-GSK3 complex. GSK3 in turn phosphorylates the C-terminus domain of LRP5/6. Phosphorylated LRP5/6 has high affinity for Axin which in turn leads to accumulation of β-catenin and its translocation into the nucleus, where it acts as a transcriptional co-activator by binding to and modulating the activity of the Tcf/Lef family of DNA-binding proteins. In the absence of Wnts, β-catenin is constitutively targeted for proteolysis impairing transcriptional events [17]. In organized epithelial sheets, Wnt signaling is low but the contribution of scaffold proteins to the inhibition of the Wnt/β-catenin remains unclear and might be due to the inhibitory role of adherens junctions and apical-basal polarity complexes [18].

Very few is known about the interactomes of SCRIB and LANO which consists at the moment of 67 and 30 protein partners, respectively, with only 9 common partners (BioGRID, version 3.5). Our study uncovers the proteomes associated with SCRIB and LANO and provides, for the first time, a deep comparative analysis of protein interactomes associated to these paralogues. We also identified a protein complex associated with SCRIB, which is stabilized by the inhibition of the proteasome, and further characterized SCRIB act as negative modulator of Wnt/β-catenin signaling.

Materials and Methods

Plasmid constructs and reagents

The cDNA encoding human SCRIB and lANO were cloned into pIRES-puro-FLAG, plasmids [19]. Antibodies purchased were mouse anti-FLAG M2 (Sigma), anti-β-catenin (Santa Cruz), anti-SCRIB (Santa Cruz). The following sequences of siRNA were used to target SCRIB: SCRIB (#05) GACCGCGUCCUCUCUAUUA, SCRIB (#06) GGACGACGAGGGCGAUAUUC.

Tissue culture and transfection

HEK293T cells were grown in Dulbecco's modified Eagle medium (DMEM; Sigma) supplemented with 10% fetal bovine serum (FBS; Invitrogen) and penicillin/streptomycin (Bioshop) in a 37°C humidified incubator with 5% CO2. Stable cell lines were generated either by calcium phosphate transfection or polyethylenimine (PEI) transfection.

Immunopurification

$5x10^7$ HEK293T cells expressing either FLAG-SCRIB or FLAG-LANO were used for affinity purification procedure. Briefly, cells were lysed and solubilized in TAP lysis buffer (0.1% Igepal CA 630, 10% glycerol, 50mM Hepes-NaOH; pH 8.0, 150mM NaCl, 2mM EDTA, 2mM DTT, 10mM NaF, 0.25mM NaOVO3, 50mM β-glycerophosphate, and protease inhibitor cocktail (Calbiochem). After 30 min centrifugation at 40,000xg (18,000 rpm in a Beckman JA20 rotor), the soluble fraction was incubated overnight at 4°C with anti-FLAG M2 agarose beads (Sigma). Beads were washed with 100 volumes of TAP lysis buffer. Beads elution was performed using Laemmli buffer.

Affinity purification, immunoprecipitation and western blot

48 hour post-transfection, cells were lysed with the TAP lysis buffer and incubated at 4ºC for 1 hour to solubilize proteins. Affinity purification and immunoprecipitations were performed using anti-FLAG-M2 beads (Sigma) for 3 hours at 4°C or using 1µg of anti-SCRIB (Santa Cruz) and 20µL of protein A beds for 3 hours at 4°C. After extensive washes with lysis buffer, proteins were eluted with 2x Laemmli sample buffer and heated at 95ºC for 5 min in the presence of β-mercaptoethanol (Sigma). Whole cell lysates or purified protein samples were resolved by SDS-polyacrylamide gel electrophoresis (SDS-PAGE) and transferred onto Biotrace NT Nitrocellulose Transfer Membranes (GE Healthcare). Western blotting was performed with antibodies as indicated in the figure legends, followed by chemiluminescent detection using appropriate HRP-conjugated antibodies and the ECL (GE Healthcare) reagent.

MG132 treatment

Depending of the experiments, cells were treated with 1 µM or 10 µM MG132 for 16 h or 4 h respectively to inhibit proteasome functions.

Production of Wnt3a conditioned medium

Mouse L cells expressing Wnt3a (CRL-2647) were cultured until reaching 90% confluency. Medium was then collected and refreshed every 2 days for a total of 6 days. Mediua from different days were assayed by TopFlash assays to determine the fractions with maximal activity and subsequently used for Wnt stimulation experiments. Conditioned mediua from parental mouse L cells not producing Wnt3a (CRL-2648) were also collected and used as controls.

TopFlash reporter assays.

Lentivirus containing the TopFlash β-catenin-dependent luciferase reporter (firefly luciferase) and *Renilla* luciferase were produced and used to establish stable HEK293T and MCF10A Wnt-reporter lines. Cells were seeded on 24-well plates, followed by cDNA transfection with Lipofectamine 2000 and/or reverse transfection with Lipofectamine RNAiMax for siRNA experiments. For experiments involving Wnt stimulation, the medium was replaced with a 1:1 mix of fresh DMEM-Wnt3a or DMEM-control conditioned medium. The cells were then assayed 24 h after stimulation in accordance with the dual luciferase assay protocol (Promega) using a plate reader (Berthold LB960).

Immunocytochemistry and confocal microscopy

HEK293T cells were grown on poly-D-Lysine (Sigma) treated coverslip and transfected as described in the figure legends. 48 hour post-transfection, cells were fixed in 4% paraformaldehyde, permeabilized with 0.2% Triton X-100 in phosphate buffered saline (PBS) and the non-specific sites were saturated with a 3% BSA (Euromedex) solution in PBS. Samples were immuno-stained with anti-SCRIB (Santa Cruz) or anti-β-catenin (Santa Cruz) antibodies or Phalloidin (Thermo) in 3% BSA. Cells were subsequently labeled with secondary (Thermo) goat anti-goat or mouse antibodies conjugated to Alexa Fluor 488 and Alexa Fluor 594 respectively. Coverslips were mounted and sealed onto slides using ProlongGold antifade reagent with DAPI mounting media (Thermo). Cells were then visualized and images acquired with a Carl Zeiss LSM880 confocal microscope using a Plan-Apochromat 63X oil immersion objective. Lasers at 488nm, 543nm and 633nm were triggered independently using the multi-track function of LSM880. Uncompressed images were processed using Zeiss LSM Image browser version ZEN.

Mass spectrometry analysis.

Protein extract were loaded on acrylamide gels to stack proteins in a single band that was stained and cut from the gel. Gels pieces were submitted to an in-gel trypsin digestion[1]. Peptides were collected, dried-down and reconstituted with 0.1% trifluoroacetic acid in 4% acetonitrile and analyzed by liquid chromatography (LC)-tandem mass spectrometry (MS/MS) using a LTQ-Orbitrap Velos Mass Spectrometer (Thermo Electron, Bremen, Germany) or using an Orbitrap Fusion Lumos Tribrid Mass Spectrometer (Thermo Electron, Bremen, Germany) both online with a nanoRSLC Ultimate 3000 chromatography system (Dionex, Sunnyvale, CA). Peptides were separated using a two steps linear gradient (4-45% acetonitrile/H_2O; 0.1 % formic acid for 120 min (see supplementary Materials and Methods for detailed methods).

Protein identification and quantification.

Relative intensity-based label-free quantification (LFQ) and iBAQ intensity were processed using the freely available MaxQuant computational proteomics platform, version 1.6.2.1. [20-22] Spectra were searched against the human database subset of the Swiss-Prot database (date 18/09/19, 20394 entries) supplemented with a set of frequently observed contaminants and using mainly default parameters. The false discovery rate (FDR) at the peptide and protein levels were set to 1%. The statistical analysis was done with Perseus program (version 1.6.1.3) [23]. To determine whether a given detected protein was specifically differential a two-sample t-test were done using permutation based FDR-controlled at 0.01 and employing 250 permutations. The differential proteomics analysis was carried out on identified proteins after removal of proteins only identified with modified peptides, peptides shared with other proteins, proteins from contaminant database and proteins which are present in 100% in at least one condition. Alternatively, The iBAQ (Intensity Based Absolute Quantification) were uploaded from the proteinGroups.txt file and transformed by a base logarithm 2 to obtain a

normal distribution. Thus, iBAQ intensities are roughly proportional to the molar quantities of the proteins.

Proteome analysis

Gene ontology (GO) and enrichment analyses were performed using the database for annotation, visualization, and integrated discovery (DAVID 6.8) [24, 25] using the full dataset as background. Interaction network were generated using STRING's website (version 11.0) at high confidence (0.7) and network is clustered to a specified "MCL inflation parameter = 3" [26, 27]. BioGRID version 3.5.171 was used to extract known SCRIB and LANO interactors [28] [29] [28]. The mass spectrometry proteomics data, including search results, have been deposited to the ProteomeXchange Consortium (www.proteomexchange.org) *via* the PRIDE[30] partner repository with the dataset identifier PXD013636 and PXD013647.

They can be accessed for reviewing purposes with the following login details :

Project accession: PXD013636; Username: reviewer40726@ebi.ac.uk; Password: qMsz4H9A

Project accession: PXD013647; Username: reviewer18814@ebi.ac.uk; Password: y93bdeTJ

Results

Protein landscapes associated to LANO and SCRIB

SCRIB and *LANO* are paralogue genes that encode proteins sharing 72% sequence homology (**Fig 1A**). To further study their functions and highlight possible differences and commonalities in term of partners, we used an unbiased proteomic approach to characterize their associated protein complexes. We first generated stable HEK293T cell lines expressing either FLAG-SCRIB or FLAG-LANO. To identify binding partners of SCRIB and LANO, we used a variation of a previously described methodology [31] based on LC-MS/MS analysis of FLAG immunoprecipitates from HEK293T cell extracts expressing either FLAG-SCRIB or FLAG-LANO or FLAG alone. Proteins identified from HEK293T cells expressing FLAG alone were compatred to proteins associated to either FLAG-SCRIB or FLAG-LANO. 3.5% of the 390 proteins found associated with SCRIB were already known as SCRIB partners in BioGRID, among them a subset of proteins previously characterized by our laboratory and others including ARGHEF7 [32], PAK [33] and SHOC2 [34], validating our approach (**Fig. 1B** and **Table S1**). Similarly, we identified 474 proteins associated with LANO (**Fig.1C** and **Table S1**). Of these, 2% were known LANO interacting partners in BioGRID (**Fig. 1C** and **Table S2**). We found that SCRIB was present in the LANO protein complex and conversely that LANO was present in the SCRIB protein complex. We validated these results by conducting co-immunoprecipitation assays followed by western blot analysis. We used stable cell lines expressing either FLAG-SCRIB or FLAG-LANO. After cell lysis and immunoprecipitation using α-FLAG antibody, we monitored the presence of LANO and SCRIB using a specific antibody able to recognize the LRR domains of the two paralogs. We found that LANO co-immunoprecipitates with SCRIB confirming our MS results (**Fig. 1D**). We next analyzed our data set to discriminate common and specific proteins bound to either SCRIB or LANO (**Fig. 1E** and **Table S3**). 30% proteins are common to SCRIB and LANO

whereas 275 are specifically associated to LANO and 191 specifically associated to SCRIB (**Fig. 1E** and **Table S4**). Several PDZ domain containing proteins were found in the SCRIB and LANO interactomes. 6 proteins (DVL2, PDLIM7, TJP2, ARHGAP21, MAGI1, MPP2) were common to the two paralogues whereas 4 were specific to LANO (DLG1, CASK, MPP7, LIN7C and and SNX27) and 5 to SCRIB (PDZ8, GOPC, SIPA1L1, SIPA1L2, SIPA1L3, PTPN13) (**Fig. 1C and Fig. 1E and Table S1 and Table S2**). We confirmed in particular our previous findings showing that DLG1 is a specific LANO partner [35].

Taken together, we provide the most exhaustive list of proteins associated with either SCRIB or LANO and show that SCRIB and LANO bind to common and different proteins.

SCRIB is associated with the β-catenin destruction complex

It has been recently shown that SCRIB acts in the HIPPO pathway by scaffolding β-TRCP1, promoting TAZ degradation at the plasma membrane of epithelial cells [7]. We did not observe the presence of either TAZ or β-TRCP1 among the SCRIB associated proteins. We then asked whether this could be due to protein degradation and thus carried out our proteomic approach after treatment of FLAG-SCRIB expressing HEK293T cells with MG132, a proteasome inhibitor. We compared the list of SCRIB-associated proteins under DMSO or MG132 treatments. We did not observe any variation of SCRIB expression by MS analysis (**Fig.2A** and **Table S5**) or western blot analysis (data not shown) suggesting that SCRIB is a relatively stable protein, poorly sensitive to proteasomal degradation. However, we found that 37 proteins were differentially associated to SCRIB upon inhibition of the proteasome (11 down-regulated and 26 up-regulated proteins). Among the partners, we identified β-catenin as a protein specifically associated with SCRIB under MG132 treatment (**Fig 2A**). Using David bioinformatic resources [24, 25], we also observed an enrichment of a subset of proteins associated to SCRIB that are involved in Wnt/β-catenin signaling, in

particular members of the β-catenin destruction complex which includes APC, Axin, AMER1, DVL and GSK3β (**Fig. 2B**). Further analysis using STRING 'functional protein association networks' [26] highlighted a protein-protein association network associated to SCRIB (**Fig. 2C**). We thus evidence a highly connected network of 17 proteins associated to SCRIB which comprise 10 proteins involved in Wnt/ß-catenin signaling (**Fig. 2B**).

Wnt3a stimulation promotes SCRIB association with β-catenin

To confirm the mass spectrometry data, we conducted immunoprecipitation of endogenous SCRIB using specific antibody, and monitored the presence of endogenous β-catenin by western blot analysis. We observed that SCRIB and β-catenin association was promoted under MG132 treatment at two different time points and at two different concentrations (**Fig 3A**). We also observed a modification of the migration pattern of β-catenin in polyacrylamide gels which is typical of ubiquitinated forms, suggesting that SCRIB might promote degradation of β-catenin through its association with the destruction complex (**Fig. 3A**). As the destruction complex is inhibited by Wnt stimulation, we next stimulated cells overnight with Wnt3a conditioned media and conducted immunoprecipitation of endogenous SCRIB and looked at the presence of β-catenin in the SCRIB complex. We observed that Wnt3a stimulation promotes the association between SCRIB and β-catenin by 1.8 fold (**Fig. 3B**). To further confirm this observation, we treated cells with LiCl, an inhibitor of GSK3β leading to β-catenin stabilization, and assessed endogenous SCRIB/β-catenin co-immunoprecipitation. We observed that the association between SCRIB and β-catenin is potentiated when GSK3β is inhibited, suggesting that this interaction is regulated by activation of Wnt/β-catenin signaling (**Fig. 3C**). We further assessed the colocalization between SCRIB and β-catenin in HEK 293T cells by immunofluorescence. We observed that

both proteins colocalize at the plasma membrane with no difference in their subcellular localization following Wnt3a conditioned media or LiCl treatments (**Fig. 3D**). Taken together, our data suggest that SCRIB is associated with β-catenin under basal conditions. However, this interaction is promoted when β-catenin is stabilized by Wnt3a or LiCl treatments.

SCRIB is a negative regulator of the Wnt/β-catenin signaling

Since SCRIB is associated with β-catenin and this interaction is modulated by Wnt3a stimulation, we next asked whether SCRIB can act as a modulator of Wnt/β-catenin signaling. We first screened siRNAs able to downregulate SCRIB in human cells. We identified two independent siRNAs able to decrease SCRIB expression by at least 50% (**Fig. 4A**). HEK293T and MCF10A cell lines stably expressing a β-catenin luciferase reporter and a *Renilla* luciferase control protein were then transfected with either control or SCRIB siRNAs. In the control transfected MCF10A and HEK293T cells, addition of Wnt3a led to 7- and 71-fold activity of the reporter, respectively, (**Fig. 4B and Fig. 4C**) compared to cells treated with control conditioned medium. Depletion of SCRIB led to an increase in Wnt3a-mediated activation by 21- and 170-fold in MCF10A and HEK293T cells, respectively (**Fig. 4B and Fig. 4C**). We therefore conclude that SCRIB acts as a negative regulator of Wnt signaling. It has been previously shown that SCRIB associates to β-catenin through its PDZ domains [36]. To further investigate the role of SCRIB as a negative regulator of Wnt/β-catenin signaling, we overexpressed full length SCRIB fused to GFP in HEK293T cells and observed a partial decrease of activity of the luciferase reporter (**Fig. 4D**). However, when we overexpressed a mutant form of SCRIB lacking its PDZ domains (GFP-SCRIBΔPDZ), we did not observe any difference with control conditions, confirming that the PDZ domains of SCRIB are required for its repressive function (**Fig. 4D**). Expression levels of GFP-SCRIB and GFP-SCRIBΔPDZ were controlled by western blot analysis (**Fig. 4E**). Together our data

demonstrate the importance of SCRIB as a negative regulator of Wnt/β-catenin signaling, probably through its direct interaction with β-catenin.

Discussion

We and others have demonstrated the importance of SCRIB and LANO in cancer development [4, 9, 13, 37]. In this study, we identified large protein complexes associated with these two paralogs and carried out for the first-time a direct comparison of their associated protein complexes. Using an established functional proteomic approach, our results show that SCRIB and LANO interact with a common set of 199 proteins. Furthermore, we demonstrate that LANO, which has high sequence homology with SCRIB in its N-terminal region (**Fig. 1A**), interacts with a specific set of 275 proteins which include 4 PDZ domain-containing proteins (DLG1 CASK, MPP7, and SNX27) and SCRIB with 191 specific partners which include 6 PDZ containing proteins (PDZ8, GOPC, SIPA1L1, SIPA1L2, SIPA1L3, PTPN13). We further characterized proteins associated with SCRIB in conditions where we inhibited proteasome activity and found that this treatment led to the association between SCRIB and the β-catenin destruction complex. Further analysis revealed that SCRIB is a negative regulator of the Wnt/β-catenin signaling pathway. Our data suggest that SCRIB scaffolds components of the destruction complex and most probably inhibits the membrane pool of β-catenin (**Fig. 3D**). Indeed, downregulation of SCRIB expression promotes an increase of Wnt/β-catenin signaling using reporter assays. In conclusion, our data suggest that SCRIB may control Wnt signaling in epithelial cells.

Our study deciphers, for the first time, the protein complexes associated with proteins encoded by the two close paralogues *SCRIB* and *LANO*. We demonstrate that SCRIB and LANO can associate since specific LANO peptides have been identified by LC-MS in the SCRIB complex (**Fig. 1B**) and conversely that specific SCRIB peptides were found in the

LANO complex (**Fig. 1C**). The SCRIB-LANO interaction was further confirmed by coimmunoprecipitation (**Fig. 1D**). Interestingly, we have recently demonstrated that LANO and SCRIB colocalize at the basolateral membranes of epithelial cells [38]. LANO harbors a C-terminal PDZ binding motif which allows its interaction with a subset of PDZ domain-containing proteins including DLG1, SNX27 or SCRIB (**Fig. 1A**) [1]. Although contribution of LANO to SCRIB functions or vice-versa has not yet been studied, we show here and in a recent report [38] that both proteins negatively regulate Wnt/β-catenin signaling suggesting overlapping functions. Our extensive analysis of their associated protein complexes will help in the future at a better understanding of their respective role in epithelial cells. Interestingly, *Scrib* knock out mice display morphogenetic defects [39] whereas *Lano* deficient mice are viable and fertile with no obvious phenotype [38]. These genetic results suggest that the two paralogues contribute differently to murine embryonic development and, combined to the results of our comparative interactomes, that SCRIB and LANO have probably both redundant and non-redundant functions. It would be of great interest in the future to cross *scrib* and *lano* deficient mice and assess a possible functional interaction between these genes.

A functional proteomic approach has been used to demonstrate that SCRIB is associated with a specific protein complex involved in Wnt/β-catenin signaling pathway. Our results suggest that SCRIB is a negative modulator of Wnt/β-catenin signaling. It has been recently shown that SCRIB, when localized at the plasma membrane, recruits β-TRCP, an E3-ubiquitin ligase that promotes degradation of TAZ in a proteasome-dependent manner, leading to inhibition of the HIPPO signaling pathway [7]. Furthermore, TAZ is also a component of the β-catenin destruction complex which, through recruitment of β-TRCP, degrades β-catenin [40]. Our initial proteomic approach done under basal conditions (**Fig. 1B**) failed to identify components of HIPPO or Wnt signaling pathways associated to SCRIB. However, by coimmunoprecipitation and western blot analysis of endogenous SCRIB, we could recover a

SCRIB/β-catenin (**Fig. 3**) but not SCRIB/TAZ complex (data not shown) suggesting that very few β-catenin is associated to SCRIB under basal conditions. Under MG132 treatment, we were able to easily identify by mass spectrometry β-catenin and members of the β-catenin (but still not TAZ) destruction complex associated with SCRIB demonstrating that, at least in our cellular model systems, the SCRIB/β-catenin destruction complex is predominant and regulated directly or indirectly by proteosomal degradation. We next showed that SCRIB behaves as a negative modulator of this signaling pathway as it does with AKT, ERK or HIPPO pathways (**Fig. 4B**). It has been recently shown that LANO represses Wnt/β-catenin signaling and promotes the maintenance of breast cancer stem cells [38]. It would be interesting to assess a possible functional cooperation between the two paralogues in this setting (**Fig 1D**).

Finally, β-catenin is a central component of the cadherin cell adhesion complex and plays an essential role in the maintenance of the epithelial structures [41]. Studies have shown that SCRIB subcellular localization is altered in colorectal carcinoma and correlates with intracellular accumulation of β-catenin compared to normal adjacent epithelia [42]. Furthermore, it has been recently shown that SCRIB is required for β-catenin localization at the plasma membrane in order to maintain the integrity of tight junctions [36]. Our findings suggest that deregulation of expression of SCRIB may potentiate Wnt/β-catenin signaling and promotes cancer development.

Figure legends

Figure 1 Protein landscapes associated to SCRIB and LANO

(A) Topology of SCRIB and LANO showing sequence homologies. **(B-C)** Mass spectrometry analysis of the protein complexes after FLAG immunopurification of proteins from HEK293T cells expressing FLAG-SCRIB **(B)** or FLAG-LANO **(C)**. Volcano plots showing differential Log2(iBAQ intensity) levels (x axis) and –Log(p-value) (y axis) for SCRIB versus control **(B)** and LANO versus control **(C).** The full lines are indicative of significant hits obtained at a Log2 difference of 2 and a –Log p-value of 2 and are highlighted in green for FLAG-SCRIB versus control conditions **(B)**, in red for FLAG-LANO versus control conditions **(C)** and in grey for proteins with non-significant changes. **(D)** Immunopurification of FLAG-SCRIB (lane 3) or FLAG-LANO (lane 4) extracted from HEK293T cell lysates using anti-FLAG antibody coupled to sepharose beads allows the identification of a SCRIB (red arrow)-LANO (green arrow) interaction. Expression of FLAG-SCRIB and FLAG-LANO in lysates are shown lane 1 and lane 2 respectively**(E)** Venn diagram showing number of total proteins (n) or PDZ domain proteins (n (PDZ)) associated to SCRIB and/or LANO. **(B-C)** Known SCRIB and LANO interactors indexed in BioGRID are highlighted in red and PDZ proteins are highlighted in orange.

Figure 2 SCRIB associates to the β-catenin destruction complex

A) Volcano plots showing differential Log2(LFQ intensity) levels (x axis) and –Log(p-value) (y axis) for proteins associated to SCRIB under DMSO or MG132 treatments. The dotted lines are indicative of significant hits obtained at a Log2 difference of 2 and a –Log p-value of 2 and are highlighted in blue for FLAG-SCRIB under DMSO vs MG132 treatments. Grey spots correspond to proteins with non-significant changes. Of note, we did not observe variation of SCRIB expression by MS analysis following MG132 treatment. **(B)** Top

Biological process enrichment using proteins found regulated under MG132 treatment vs DMSO using a biocomputational tool (DAVID). **(C)** Scheme of functional protein networks using STRING's website with the SCRIB-associated proteins regulated by MG132 treatment and including SCRIB as bait. One main cluster (red) with highly connected proteins (green and blue) is shown.

Figure 3 Wnt3a stimulation promotes SCRIB association with β-catenin

(A-C) Immunopurification of endogenous SCRIB and presence of β-catenin in the complex was assessed by western blot analysis. Before lysis, cells were treated with MG132 for the indicated times and concentrations **(A)**. Cells were treated with Ctl- or Wnt3a-condition media for 16 hours before lysis **(B).** Cells were treated with 10mM LiCl or 10mM NaCl for 16 hours before lysis **(C)**. **(D)** HEK 293T cells were seeded on Poly-L-Lysine coverslips and treated with 10mM NaCl, 10mM LiCl, Ctl-CM or Wnt3a-CM for 16 hours. After fixation, cells were stained with phalloidin (purple) to reveal polymerized actin, anti-SCRIB antibody (green), anti-β-catenin antibody (red) and DAPI (blue). Scale bars 20 μM.

Figure 4 SCRIB is a negative regulator of Wnt/β-catenin signaling

(A) Two independent siRNAs targeting SCRIB or a control siRNA (Non-Targeting, NT) were transfected into HEK 293T cells. Decrease of SCRIB expression was confirmed by western blot analysis. **(B-C)** MCF10A **(B)** or HEK 293T **(C)** cells stably expressing the TOP Flash luciferase reporter were transfected with the indicated siRNAs and, after 24 hours, were treated with either WT-CM or Wnt3a-CM for 16 hours. The luciferase reporter activity was measured with a luminometer (mean ± standard deviation; n = 3). **(D)** HEK 293T cells transfected with the indicated constructs were treated with WT-CM or Wnt3a-CM for 16 hours. Expression of GFP-SCRIB constructs was assessed by western blot analysis **(E)**.

References

[1] Santoni, M. J., Pontarotti, P., Birnbaum, D., Borg, J. P., The LAP family: a phylogenetic point of view. *Trends Genet* 2002, *18*, 494-497.

[2] Bilder, D., Li, M., Perrimon, N., Cooperative regulation of cell polarity and growth by Drosophila tumor suppressors. *Science* 2000, *289*, 113-116.

[3] Qin, Y., Capaldo, C., Gumbiner, B. M., Macara, I. G., The mammalian Scribble polarity protein regulates epithelial cell adhesion and migration through E-cadherin. *J Cell Biol* 2005, *171*, 1061-1071.

[4] Navarro, C., Nola, S., Audebert, S., Santoni, M. J., *et al.*, Junctional recruitment of mammalian Scribble relies on E-cadherin engagement. *Oncogene* 2005, *24*, 4330-4339.

[5] Li, X., Yang, H., Liu, J., Schmidt, M. D., Gao, T., Scribble-mediated membrane targeting of PHLPP1 is required for its negative regulation of Akt. *EMBO Rep* 2011, *12*, 818-824.

[6] Nagasaka, K., Massimi, P., Pim, D., Subbaiah, V. K., *et al.*, The mechanism and implications of hScrib regulation of ERK. *Small GTPases* 2010, *1*, 108-112.

[7] Cordenonsi, M., Zanconato, F., Azzolin, L., Forcato, M., *et al.*, The Hippo transducer TAZ confers cancer stem cell-related traits on breast cancer cells. *Cell* 2011, *147*, 759-772.

[8] Feigin, M. E., Akshinthala, S. D., Araki, K., Rosenberg, A. Z., *et al.*, Mislocalization of the cell polarity protein scribble promotes mammary tumorigenesis and is associated with basal breast cancer. *Cancer Res* 2014, *74*, 3180-3194.

[9] Zhan, L., Rosenberg, A., Bergami, K. C., Yu, M., *et al.*, Deregulation of scribble promotes mammary tumorigenesis and reveals a role for cell polarity in carcinoma. *Cell* 2008, *135*, 865-878.

[10] Nakagawa, S., Huibregtse, J. M., Human scribble (Vartul) is targeted for ubiquitin-mediated degradation by the high-risk papillomavirus E6 proteins and the E6AP ubiquitin-protein ligase. *Mol Cell Biol* 2000, *20*, 8244-8253.

[11] Arpin-Andre, C., Mesnard, J. M., The PDZ domain-binding motif of the human T cell leukemia virus type 1 tax protein induces mislocalization of the tumor suppressor hScrib in T cells. *J Biol Chem* 2007, *282*, 33132-33141.

[12] Thomas, M., Massimi, P., Navarro, C., Borg, J. P., Banks, L., The hScrib/Dlg apico-basal control complex is differentially targeted by HPV-16 and HPV-18 E6 proteins. *Oncogene* 2005, *24*, 6222-6230.

[13] Elsum, I. A., Yates, L. L., Pearson, H. B., Phesse, T. J., *et al.*, Scrib heterozygosity predisposes to lung cancer and cooperates with KRas hyperactivation to accelerate lung cancer progression in vivo. *Oncogene* 2014, *33*, 5523-5533.

[14] Wu, M., Pastor-Pareja, J. C., Xu, T., Interaction between Ras(V12) and scribbled clones induces tumour growth and invasion. *Nature* 2010, *463*, 545-548.

[15] Steinhart, Z., Angers, S., Wnt signaling in development and tissue homeostasis. *Development* 2018, *145*.

[16] Zhan, T., Rindtorff, N., Boutros, M., Wnt signaling in cancer. *Oncogene* 2017, *36*, 1461-1473.

[17] Angers, S., Moon, R. T., Proximal events in Wnt signal transduction. *Nat Rev Mol Cell Biol* 2009, *10*, 468-477.

[18] Basu, S., Cheriyamundath, S., Ben-Ze'ev, A., Cell-cell adhesion: linking Wnt/beta-catenin signaling with partial EMT and stemness traits in tumorigenesis. *F1000Res* 2018, *7*.

[19] Angers, S., Thorpe, C. J., Biechele, T. L., Goldenberg, S. J., *et al.*, The KLHL12-Cullin-3 ubiquitin ligase negatively regulates the Wnt-beta-catenin pathway by targeting Dishevelled for degradation. *Nat Cell Biol* 2006, *8*, 348-357.

[20] Cox, J., Hein, M. Y., Luber, C. A., Paron, I., *et al.*, Accurate proteome-wide label-free quantification by delayed normalization and maximal peptide ratio extraction, termed MaxLFQ. *Mol Cell Proteomics* 2014, *13*, 2513-2526.

[21] Cox, J., Mann, M., MaxQuant enables high peptide identification rates, individualized p.p.b.-range mass accuracies and proteome-wide protein quantification. *Nat Biotechnol* 2008, *26*, 1367-1372.

[22] Cox, J., Neuhauser, N., Michalski, A., Scheltema, R. A., *et al.*, Andromeda: a peptide search engine integrated into the MaxQuant environment. *J Proteome Res* 2011, *10*, 1794-1805.

[23] Schwanhausser, B., Busse, D., Li, N., Dittmar, G., *et al.*, Global quantification of mammalian gene expression control. *Nature* 2011, *473*, 337-342.

[24] Huang da, W., Sherman, B. T., Lempicki, R. A., Systematic and integrative analysis of large gene lists using DAVID bioinformatics resources. *Nat Protoc* 2009, *4*, 44-57.

[25] Huang da, W., Sherman, B. T., Lempicki, R. A., Bioinformatics enrichment tools: paths toward the comprehensive functional analysis of large gene lists. *Nucleic Acids Res* 2009, *37*, 1-13.

[26] Szklarczyk, D., Gable, A. L., Lyon, D., Junge, A., *et al.*, STRING v11: protein-protein association networks with increased coverage, supporting functional discovery in genome-wide experimental datasets. *Nucleic Acids Res* 2019, *47*, D607-D613.

[27] von Mering, C., Jensen, L. J., Snel, B., Hooper, S. D., *et al.*, STRING: known and predicted protein-protein associations, integrated and transferred across organisms. *Nucleic Acids Res* 2005, *33*, D433-437.

[28] Stark, C., Breitkreutz, B. J., Reguly, T., Boucher, L., *et al.*, BioGRID: a general repository for interaction datasets. *Nucleic Acids Res* 2006, *34*, D535-539.

[29] Oughtred, R., Stark, C., Breitkreutz, B. J., Rust, J., *et al.*, The BioGRID interaction database: 2019 update. *Nucleic Acids Res* 2019, *47*, D529-D541.

[30] Vizcaino, J. A., Deutsch, E. W., Wang, R., Csordas, A., *et al.*, ProteomeXchange provides globally coordinated proteomics data submission and dissemination. *Nat Biotechnol* 2014, *32*, 223-226.

[31] Daulat, A. M., Luu, O., Sing, A., Zhang, L., *et al.*, Mink1 regulates beta-catenin-independent Wnt signaling via Prickle phosphorylation. *Mol Cell Biol* 2012, *32*, 173-185.

[32] Audebert, S., Navarro, C., Nourry, C., Chasserot-Golaz, S., *et al.*, Mammalian Scribble forms a tight complex with the betaPIX exchange factor. *Curr Biol* 2004, *14*, 987-995.

[33] Nola, S., Sebbagh, M., Marchetto, S., Osmani, N., *et al.*, Scrib regulates PAK activity during the cell migration process. *Hum Mol Genet* 2008, *17*, 3552-3565.

[34] Young, L. C., Hartig, N., Munoz-Alegre, M., Oses-Prieto, J. A., *et al.*, An MRAS, SHOC2, and SCRIB complex coordinates ERK pathway activation with polarity and tumorigenic growth. *Mol Cell* 2013, *52*, 679-692.

[35] Saito, H., Santoni, M. J., Arsanto, J. P., Jaulin-Bastard, F., *et al.*, Lano, a novel LAP protein directly connected to MAGUK proteins in epithelial cells. *J Biol Chem* 2001, *276*, 32051-32055.

[36] Gujral, T. S., Karp, E. S., Chan, M., Chang, B. H., MacBeath, G., Family-wide investigation of PDZ domain-mediated protein-protein interactions implicates beta-catenin in maintaining the integrity of tight junctions. *Chem Biol* 2013, *20*, 816-827.

[37] Wan, S., Meyer, A. S., Weiler, S. M. E., Rupp, C., *et al.*, Cytoplasmic localization of the cell polarity factor scribble supports liver tumor formation and tumor cell invasiveness. *Hepatology* 2018, *67*, 1842-1856.

[38] Lopez Almeida, L., Sebbagh, M., Bertucci, F., Finetti, P., *et al.*, The SCRIB Paralog LANO/LRRC1 Regulates Breast Cancer Stem Cell Fate through WNT/beta-Catenin Signaling. *Stem Cell Reports* 2018, *11*, 1040-1050.

[39] Montcouquiol, M., Rachel, R. A., Lanford, P. J., Copeland, N. G., *et al.*, Identification of Vangl2 and Scrb1 as planar polarity genes in mammals. *Nature* 2003, *423*, 173-177.

[40] Azzolin, L., Panciera, T., Soligo, S., Enzo, E., *et al.*, YAP/TAZ incorporation in the beta-catenin destruction complex orchestrates the Wnt response. *Cell* 2014, *158*, 157-170.

[41] Nelson, W. J., Nusse, R., Convergence of Wnt, beta-catenin, and cadherin pathways. *Science* 2004, *303*, 1483-1487.

[42] Kamei, Y., Kito, K., Takeuchi, T., Imai, Y., *et al.*, Human scribble accumulates in colorectal neoplasia in association with an altered distribution of beta-catenin. *Hum Pathol* 2007, *38*, 1273-1281.

Conflict of interest statement

The authors have no conflict of interest to declare.

Acknowledgements

This work was funded by La Ligue Nationale Contre le Cancer (Label Ligue JPB, and fellowship to AMD), Fondation de France (fellowship to AMD), Fondation ARC pour la Recherche sur le Cancer (grant to JPB), and SIRIC (INCa-DGOS-Inserm 6038, fellowship to AMD). M.S.W. is a recipient of the Science without Borders PhD program from Brazil Coordenação de Aperfeiçoamento de Pessoal de Nível Superior (CAPES). A.W. is a recipient of a fellowship of Assistance Publique des Hôpitaux de Marseille. Jean-Paul Borg is a scholar of Institut Universitaire de France. Proteomic analyses were done using the mass spectrometry facility of Marseille Proteomics (marseille-proteomique.univ-amu.fr) supported by IBISA (Infrastructures Biologie Santé et Agronomie), Plateforme Technologique Aix-Marseille, Canceropôle PACA, Région Sud Provence-Alpes-Côte d'Azur, Institut Paoli-Calmettes and Fonds Européen de Développement Régional and Plan Cancer. The authors wish to thank Lena Brydon for the English editing of the manuscript and Yves Toiron for technical assistance in mass spectrometry analysis.

Authors' contributions

AMD designed the study. JPB and LC supervised the study. AMD, JPB and LC wrote the manuscript. AMD and MSW performed molecular, cellular and biochemical experiments. AW performed immunofluorescence experiments. SA, EB, LC and AMD performed the mass spectrometry analysis.

Supplementary Materials and Methods

Mass spectrometry analysis.

Protein extract were loaded on NuPAGE 4-12% Bis-Tris acrylamide gels (Life Technologies) to stack proteins in a single band that was stained with Imperial Blue (Pierce, Rockford, IL) and cut from the gel. Gels pieces were submitted to an in-gel trypsin digestion[1] with slight modifications. Briefly, gel pieces were washed and destained using 100 mM NH_4HCO_3/acetonitrile (50/50). Destained gel pieces were shrunk with acetonitrile and were re-swollen in the presence of 100 mM ammonium bicarbonate in 50% acetonitrile and dried at room temperature. Protein bands were then rehydrated and cysteines were reduced using 10 mM DTT in 100 mM ammonium bicarbonate pH 8.0 for 45 min at 56 C before alkylation in the presence of 55 mM iodoacetamide in 100 mM ammonium bicarbonate pH 8.0 for 30 min at room temperature in the dark. Proteins were then washed twice in 100 mM ammonium bicarbonate and finally shrunk by incubation for 5 min with 100 mM ammonium bicarbonate in 50% acetonitrile. The resulting alkylated gel pieces were dried at room temperature. The dried gel pieces were re-swollen by incubation in 100 mM ammonium bicarbonate pH 8.0 supplemented with trypsin (12.5 ng/µL; Promega) for 1h at 4 C and then incubated overnight at 37°C. Peptides were harvested by collecting the initial digestion solution and carrying out two extractions; first in 5% formic acid and then in 5% formic acid in 60% acetonitrile. Pooled extracts were dried down in a centrifugal vacuum system. Samples were reconstituted with 0.1% trifluoroacetic acid in 4% acetonitrile and analyzed by liquid chromatography (LC)-tandem mass spectrometry (MS/MS) using a LTQ-Orbitrap Velos Mass Spectrometer (Thermo Electron, Bremen, Germany) or using an Orbitrap Fusion Lumos Tribrid Mass Spectrometer (Thermo Electron, Bremen, Germany) both online with a nanoRSLC Ultimate 3000 chromatography system (Dionex, Sunnyvale, CA). Peptides were separated on a Dionex

Acclaim PepMap RSLC C18 column. First peptides were concentrated and purified on a pre-column from Dionex (C18 PepMap100, 2 cm × 100 µm I.D, 100 Å pore size, 5 µm particle size) in solvent A (0.1% formic acid in 2% acetonitrile). In the second step, peptides were separated on a reverse phase LC EASY-Spray C18 column from Dionex (PepMap RSLC C18, 15 or 50 cm × 75 µm I.D, 100 Å pore size, 2 µm particle size) at 300 nL/min flow rate. After column equilibration using 4% of solvent B (20% water - 80% acetonitrile - 0.1% formic acid), peptides were eluted from the analytical column by a two steps linear gradient (4-20% acetonitrile/H_2O; 0.1 % formic acid for 90 min and 20-45% acetonitrile/H_2O; 0.1% formic acid for 30 min). For peptide ionization in the EASY-Spray nanosource in front of the LTQ-Orbitrap Velos, spray voltage was set at 1.9 kV and the capillary temperature at 275°C. The Orbitrap Velos was used in data dependent mode to switch consistently between MS and MS/MS. Time between Masters MS spectra were acquired with the Orbitrap in the range of *m/z* 300-1700 at a FWHM resolution of 30 000 measured at 400 *m/z*. For internal mass calibration, the 445.120025 ion was used as lock mass. The more abundant precursor ions were selected and collision-induced dissociation fragmentation was performed in the ion trap on the 10 most intense precursor ions measured to have maximum sensitivity and yield a maximum amount of MS/MS data. The signal threshold for an MS/MS event was set to 5000 counts. Charge state screening was enabled to exclude precursors with 0 and 1 charge states. Dynamic exclusion was enabled with a repeat count of 1, exclusion list size 500 and exclusion duration of 30 s.

For peptide ionization in the EASY-Spray nanosource in front of the Orbitrap Fusion Lumos Tribrid Mass Spectrometer, spray voltage was set at 2.2 kV and the capillary temperature at 275 °C. The Orbitrap Lumos was used in data dependent mode to switch consistently between MS and MS/MS. Time between Masters Scans was set to 3 seconds. MS spectra were

acquired with the Orbitrap in the range of m/z 400-1600 at a FWHM resolution of 120 000 measured at 400 *m/z*. AGC target was set at 4.0e5 with a 50 ms Maximum Injection Time. For internal mass calibration the 445.120025 ions were used as lock mass. The more abundant precursor ions were selected and collision-induced dissociation fragmentation was performed in the ion trap to have maximum sensitivity and yield a maximum amount of MS/MS data. Number of precursor ions was automatically defined along run in 3s windows using the "Inject Ions for All Available pararallelizable time option" with a maximum injection time of 300 ms. The signal threshold for an MS/MS event was set to 5000 counts. Charge state screening was enabled to exclude precursors with 0 and 1 charge states. Dynamic exclusion was enabled with a repeat count of 1 and a duration of 60 s.

Protein identification and quantification.

Relative intensity-based label-free quantification (LFQ) and iBAQ intensity were processed using the MaxLFQ algorithm[20] from the freely available MaxQuant computational proteomics platform, version 1.6.2.1.[21] The acquired raw LC Orbitrap MS data were first processed using the integrated Andromeda search engine.[22] Spectra were searched against the human database subset of the Swiss-Prot database (date 18/09/19, 20394 entries). This database was supplemented with a set of 245 frequently observed contaminants. The following parameters were used for searches: (*i*) trypsin allowing cleavage before proline; (ii) two missed cleavages were allowed; (*ii*) monoisotopic precursor tolerance of 20 ppm in the first search used for recalibration, followed by 4.5 ppm for the main search and 0.5 Da for fragment ions from MS/MS ; (*iii*) cysteine carbamidomethylation (+57.02146) as a fixed modification and methionine oxidation (+15.99491) and N-terminal acetylation (+42.0106) as variable modifications; (*iv*) a maximum of five modifications per peptide allowed; and (*v*) minimum peptide length was 7 amino acids and a maximum mass of 4,600 Da. The match

between runs option was enabled to transfer identifications across different LC-MS/MS replicates based on their masses and retention time within a match time window of 0.7 min and using an alignment time window of 20 min. The quantification was performed using a minimum ratio count of 1 (unique+razor) and the second peptide option to allow identification of two co-fragmented co-eluting peptides with similar masses. The false discovery rate (FDR) at the peptide and protein levels were set to 1% and determined by searching a reverse database. For protein grouping, all proteins that cannot be distinguished based on their identified peptides were assembled into a single entry according to the MaxQuant rules. The statistical analysis was done with Perseus program (version 1.6.1.3) from the MaxQuant environment (www.maxquant.org). The LFQ normalised intensities or the iBAQ intensity[30] were uploaded from the ProteinGroups.txt file. The iBAQ intensities are roughly proportional to the molar quantities of the proteins. Proteins marked as contaminant, reverse hits, and "only identified by site" were discarded. Quantifiable proteins were defined as those detected in at least 100% of samples in at least one condition. Protein LFQ normalized intensities were base 2 logarithmized to obtain a normal distribution. Missing values were replaced using data imputation by randomly selecting from a normal distribution centred on the lower edge of the intensity values that simulates signals of low abundant proteins using default parameters (a downshift of 1.8 standard deviation and a width of 0.3 of the original distribution). In this way, imputation of missing values in the controls allows statistical comparison of protein abundances that are present only in the inhibitors samples. To determine whether a given detected protein was specifically differential a two-sample t-test were done using permutation based FDR-controlled at 0.01 and employing 250 permutations. The differential proteomics analysis was carried out on identified proteins after removal of proteins only identified with modified peptides, peptides shared with other proteins, proteins from contaminant database and proteins which are present in 100% in at

least one condition. Alternatively, The iBAQ (Intensity Based Absolute Quantification)[23] were uploaded from the proteinGroups.txt file and transformed by a base logarithm 2 to obtain a normal distribution. Thus, iBAQ intensities are roughly proportional to the molar quantities of the proteins.

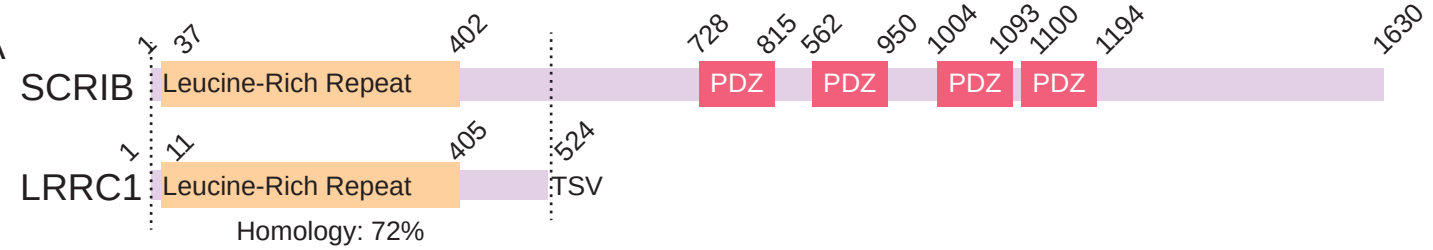
A
SCRIB
Leucine-Rich Repeat
PDZ
PDZ
PDZ
PDZ
1
37
402
728
815
562
950
1004
1093
1100
1194
1630
LRRC1
Leucine-Rich Repeat
TSV
1
11
405
524
Homology: 72%

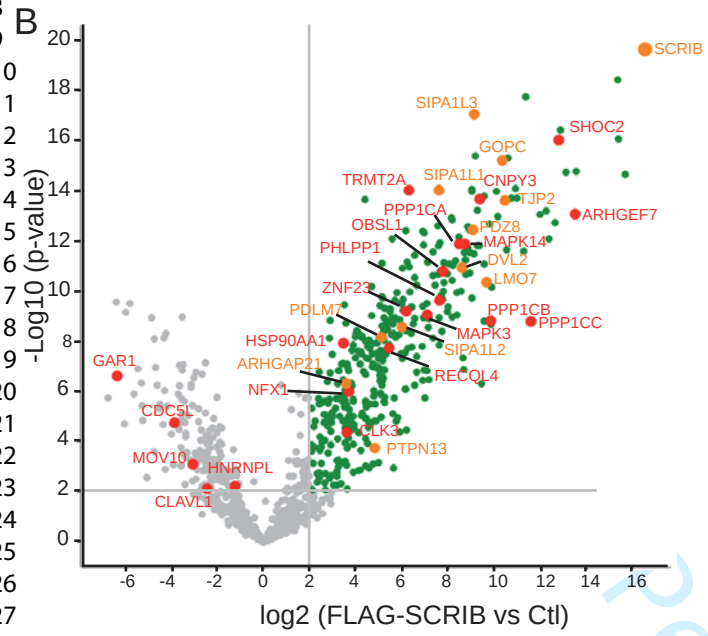
B
-Log10 (p-value)
log2 (FLAG-SCRIB vs Ctl)
SCRIB
SIPA1L3
SHOC2
GOPC
TRMT2A
SIPA1L1
CNPY3
TJP2
ARHGEF7
PPP1CA
OBSL1
PDZ8
MAPK14
PHLPP1
DVL2
LMO7
ZNF23
PDLM7
PPP1CB
PPP1CC
MAPK3
HSP90AA1
SIPA1L2
GAR1
ARHGAP21
RECQL4
NFX1
CDC5L
CLK3
PTPN13
MOV10
HNRNPL
CLAVL1

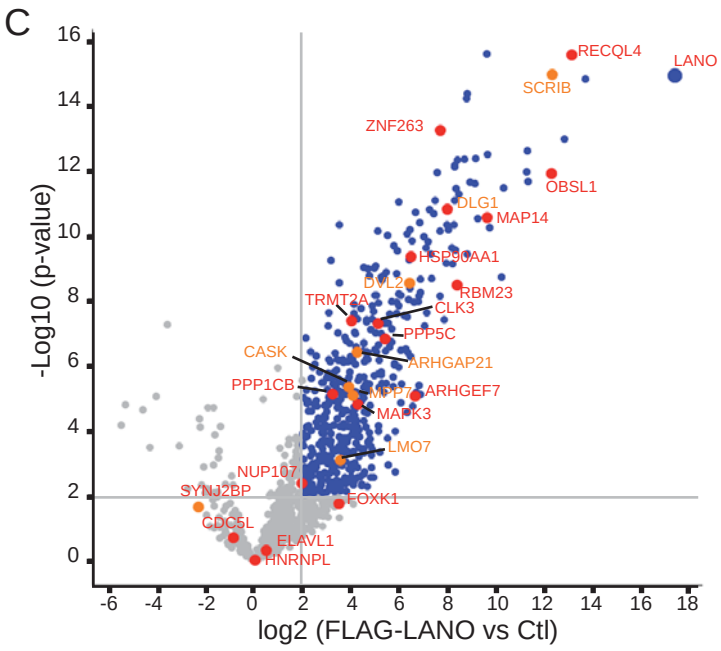
C
-Log10 (p-value)
log2 (FLAG-LANO vs Ctl)
RECQL4
LANO
SCRIB
ZNF263
OBSL1
DLG1
MAP14
HSP90AA1
DVL2
RBM23
TRMT2A
CLK3
PPP5C
CASK
ARHGAP21
PPP1CB
ARHGEF7
MAPK3
LMO7
NUP107
SYNJ2BP
FOXK1
CDC5L
ELAVL1
HNRNPL

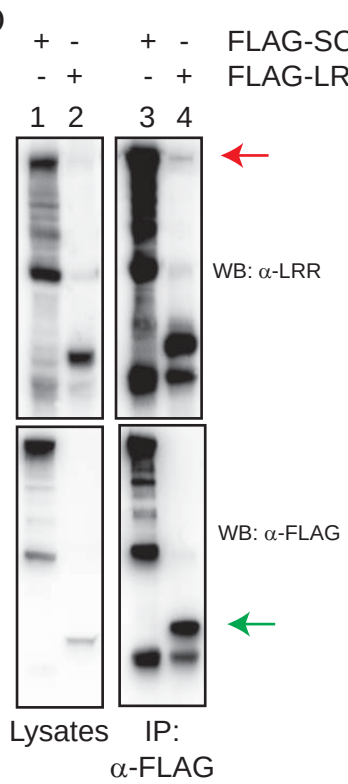
D
+ - + - FLAG-SCRIB
- + - + FLAG-LRCC1
1 2 3 4
WB: α-LRR
WB: α-FLAG
Lysates
IP:
α-FLAG

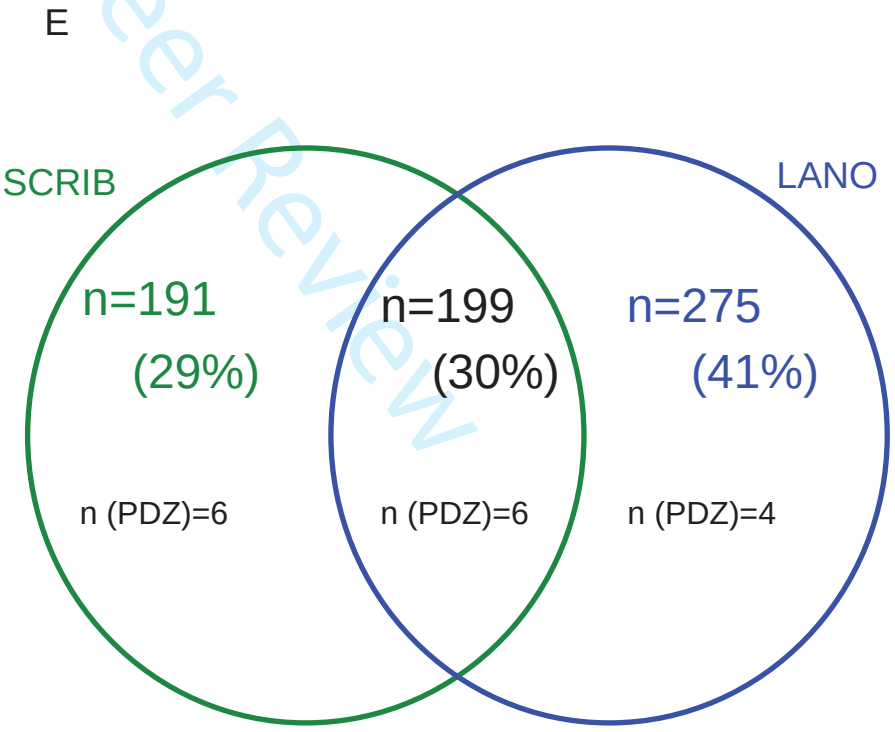
E
SCRIB
LANO
n=191
(29%)
n=199
(30%)
n=275
(41%)
n (PDZ)=6
n (PDZ)=6
n (PDZ)=4

FIGURE 2

A

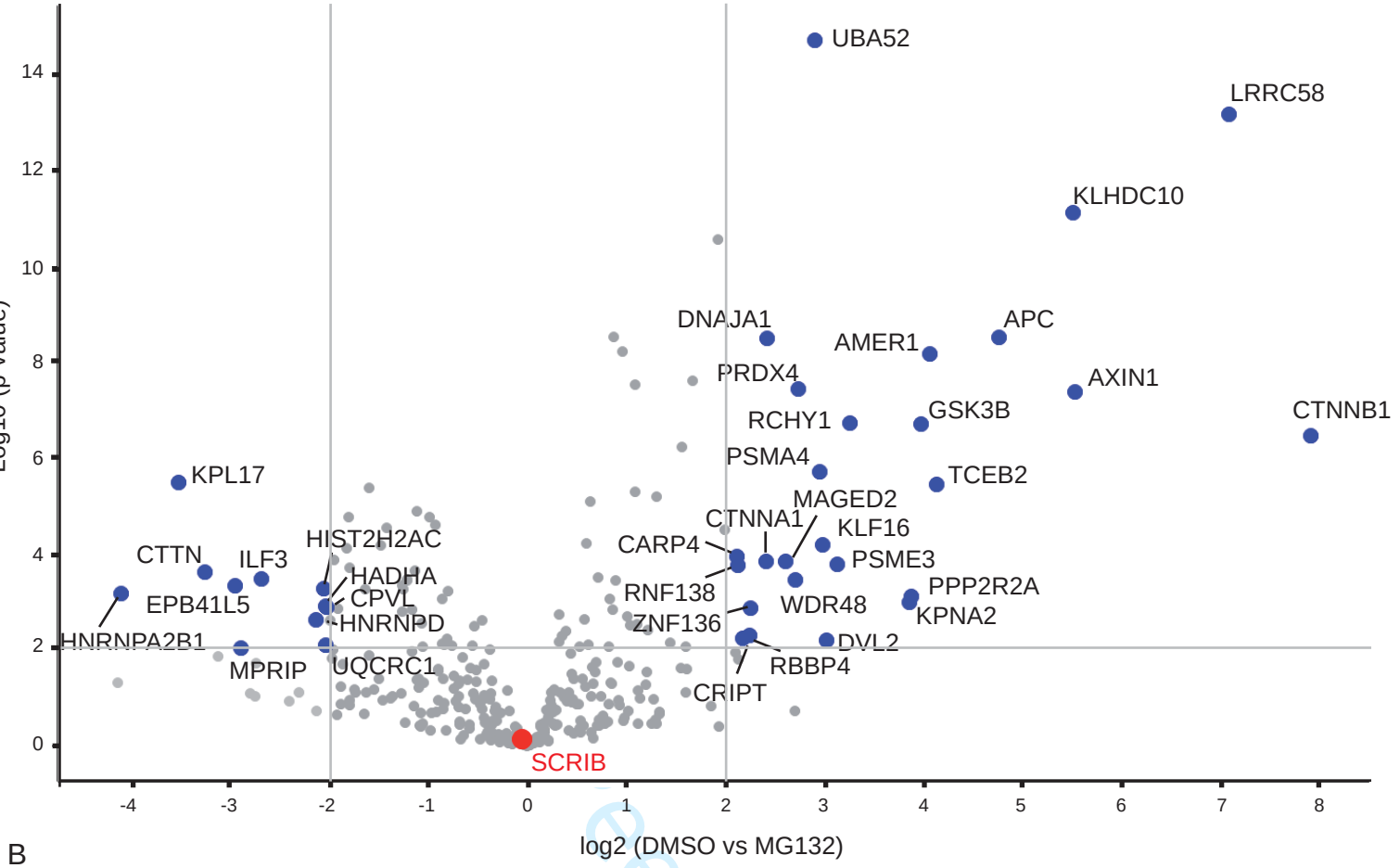

B

Biological Process term	AMER1	APC	AXIN1	CTNNB1	DVL2	GSK3B	PSME3	PSME4	RNF138	UBA52	Count	P-value
negative regulation of canonical Wnt signaling pathway	■	■	■		■	■	■	■		■	8	0.0001
proteasome-mediated ubiquitin-dependent protein catabolic process	■	■	■	■		■	■	■		■	8	0.00019
beta-catenin destruction complex disassembly	■	■	■	■	■	■					6	0.0002
Wnt signaling pathway	■	■	■	■	■	■			■	■	8	0.00084
positive regulation of canonical Wnt signaling pathway	■		■	■		■	■		■	6	0.001
canonical Wnt signaling pathway		■	■	■	■	■					5	0.0015
beta-catenin destruction complex assembly	■	■	■		■						4	0.0043
positive regulation of protein catabolic process		■	■		■						3	0.032
Wnt signaling pathway, planar cell polarity pathway					■		■	■		■	4	0.045

C

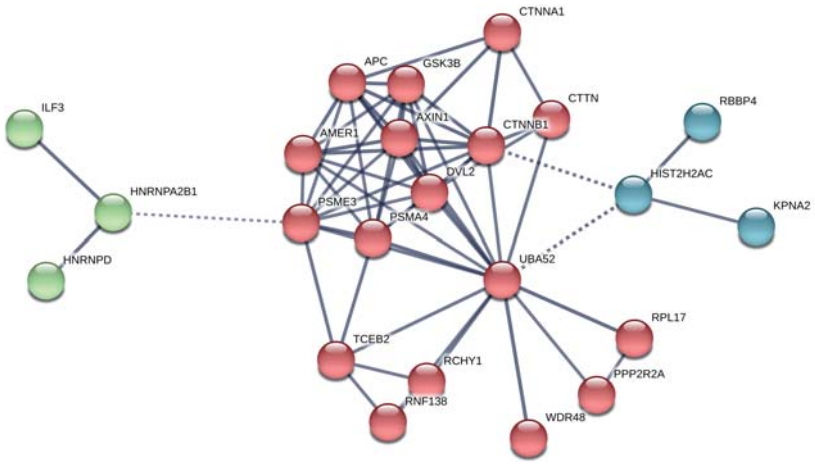

FIGURE 3

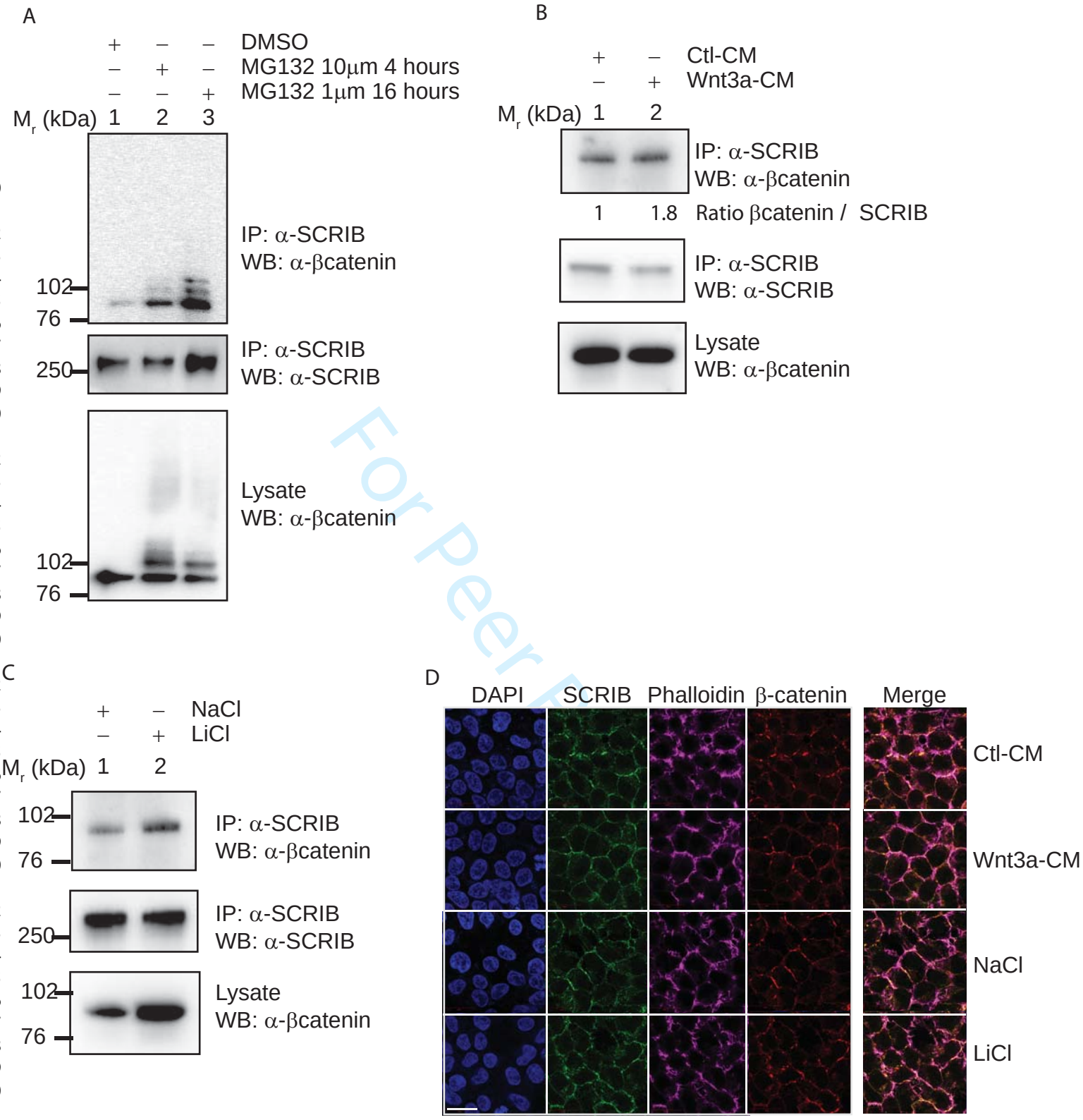

FIGURE 4